

Gradual freezing of orientational degrees of freedom in cubic $\text{Ar}_{1-x}(\text{N}_2)_x$ mixtures

M.H. Müser and P. Nielaba

Institut für Physik, Johannes-Gutenberg-Universität, KoMa 331, D-55099 Mainz, Federal Republic of Germany

(Received 9 February 1995)

The mixed crystal $\text{Ar}_{1-x}(\text{N}_2)_x$ is studied by Monte Carlo (MC) methods for $x = 0.33, 0.67,$ and 1.0 over a wide range of temperatures. For $x = 1$ we find a first-order transition from ordered cubic to disordered cubic, while for $x = 0.33$ and $x = 0.67$ we find broad nonuniform distribution functions of the local quadrupolar Edwards-Anderson order parameter at low temperatures. The short-range order of the quadrupolar mass distribution of the N_2 molecules in the mixed systems is different from that observed in the pure N_2 crystal, although the fcc symmetry has been chosen for the translational degrees of freedom. Quantum effects and the effects of the translational rotational coupling are quantified by path integral MC and classical MC, respectively.

Oriental glasses (OG's), such as $(\text{para-H}_2)_{1-x}(\text{ortho-H}_2)_x,$ $(\text{Ar})_{1-x}(\text{N}_2)_x,$ and $(\text{KBr})_{1-x}(\text{KCN})_x,$ exhibit some features which distinguish them from other types of glasses like canonical glasses or spin glasses on the one hand and molecular solids on the other hand. The main characteristic of OG's from a structural point of view is the presence of an underlying crystal lattice for the mass centers of the molecules and atoms, and the absence of a long-range order of quadrupole moments associated with the molecules even at very low-temperatures. A lot of experimental data, like diffraction spectra, low-temperature specific heat, mechanic modulus $C_{44},$ and NMR data, are available (for a review see Ref. 1) and many of these data show unusual behavior. Some of these data are interpreted in terms of computer simulation and concepts like mean field theories and random bond and random stress models (for a review see Ref. 2). Many aspects of the theoretical descriptions, however, lack a realistic microscopic modeling and even in simulations the quadrupole-quadrupole interaction is mostly realized by an *ad hoc* distribution of coupling parameters between neighbored quadrupoles, so that competing interactions are introduced analog to spin glasses.

A key quantity to microscopically characterize quadrupolar glasses (QG's) is the distribution $P(\sigma)$ of all local orientational order parameters $\sigma_i = \lim_{t \rightarrow \infty} g_i(t),$ ³ where $g_i(t)$ is the time autocorrelation function,

$$g_i(t) = \frac{3}{2} \sum_{\mu, \nu} \langle f_i^{\mu\nu}(t') f_i^{\mu\nu}(t+t') \rangle, \quad (1)$$

of the quadrupole moment tensor $f_i^{\mu\nu}(t) = n_i^\mu(t) n_i^\nu(t) - \delta^{\mu\nu}/3,$ where $n_i^\mu(t)$ is the μ th Cartesian component of the unit vector, describing the orientation of the i th molecule, and $\delta^{\mu\nu}$ being the Kronecker symbol.

The distribution $P(\sigma)$ has been obtained in an early NMR study⁴ of a hcp $\text{Ar}_{1-x}(\text{N}_2)_x$ solid mixture ($x=0.67$). Broad nonuniform distributions, smoothly evolving with the temperature, have been measured and their characteristics seem to have a general character for QG's, since quantum solid $(\text{para-H}_2)_{1-x}(\text{ortho-H}_2)_x$

shows a very similar behavior.⁵ Li *et al.*⁶ presented a phenomenological model for the distribution function $P(\sigma),$ ignoring lattice vibrations and using normally distributed site energies. The obtained distributions are qualitatively similar to the measured ones, but they also show some systematic deviations of the available experimental data. Devoret and Esteve⁷ presented a Monte Carlo (MC) study of a highly idealized model where the described behavior of $P(\sigma)$ could be found. However, only quadrupole-quadrupole interactions had been taken into account, ignoring the coupling of the orientational degrees of freedom to the translational degrees of freedom. Within this model, cooperativity of the reorientational diffusion could therefore not be found at low N_2 concentrations even at very low temperatures. Even in more recent MC studies,^{8,9} where the site-averaged Edwards-Anderson-type order parameter $\sigma_{\text{EA}} = [\sigma]_{\text{av}}$ is computed, the coupling of the molecules to each other and to the crystal field as well as to the translational degrees of freedom is treated in a rather phenomenological way. Thus computer simulations using realistic potentials are highly desirable, in order to get a more detailed microscopic understanding of the freezing-in process of quadrupole moments.

In this paper we present Monte Carlo data of unmixed and randomly mixed molecular crystals, containing linear molecules and point particles, interacting via Lennard-Jones potentials,¹⁰ whose parameters already have been used in a molecular dynamics simulation by Klee *et al.*,¹¹ resulting in a very rough estimation of the phase boundaries of the $\text{Ar}_{1-x}(\text{N}_2)_x$ mixed crystal in the T - x plane, but compatible with the experimental data. The sampled variables are the center of mass coordinates of all atoms and all molecules, as well as the orientational coordinates of every molecule. Periodic boundary conditions are chosen as cubic, according the symmetry of the Ar-rich fcc phase for $x < x_1 \approx 0.5$ as well as the symmetry of the N_2 -rich $Pa3$ phase for $x > x_2 \approx 0.8.$ ^{12,13} The concentrations $x = 0.33, 0.67$ and $x = 1$ have been investigated. The MC simulations were performed in the (N, V, T) ensemble. For $x = 0.67$ and $x = 1$ we chose $N = 4 \times 4^3;$ for $x = 0.33$ we chose $N = 4 \times 5^3.$ Such

small system sizes are sufficient to characterize the systems away from their phase boundaries. For $x = 0.33$ and $x = 0.67$ we have averaged over four sample configurations, where the Ar atoms and N_2 molecules were distributed over the available lattice sites. The lattice constant a was extrapolated linearly with x between the lattice constants a_{Ar} and a_{Pa3} , minimizing the classical potential energy of the pure Ar system and the classical potential of the pure N_2 system in the $Pa3$ phase, respectively. The orientations of the N_2 molecules have been set up according to the $Pa3$ phase. Depending on the temperature of the samples, we performed up to 4×10^5 MC steps (MCS) for equilibration and up to 1.5×10^5 MCS, where the observables have been averaged.

We first consider the case $x = 1$. At $T_1 = 35$ K the transition of disordered fcc N_2 to the long-range-ordered $Pa3-N_2$ structure takes place in the real system.¹⁴ Both phases, the cubic disordered phase at higher temperatures and the cubic long-range-ordered phase, can be stabilized for N_2 concentrations down to $x \approx 0.8$.^{15,16} For N_2 -rich systems there exist experimental and theoretical evidence for a first-order orientational order-disorder transition from $Pa3$ to fcc, due to x-ray diffraction,¹⁵ Raman scattering,¹⁶ Landau-type analysis,²² and mean field theory.¹⁷ In the hcp phase, long-range ordering of the quadrupoles does not occur, nor in the Ar-rich phase.¹³

With our choice of the potential parameters we find a transition at the temperature $T_1 = 17.5$ K. The order parameter σ changes from zero to 0.65 at T_1 . The obtained σ , internal energy, and specific heat could easily be described within the Landau-type analysis. The difference between simulated and experimental T_1 clearly originates from neglecting the interaction of the permanent electrical quadrupole of the N_2 molecules, which is nearly exactly half of the total quadrupole-quadrupole interaction. (See Ref. 18, where the phase diagram of pure N_2 could be computed in the p - T plane in very good agreement with experiment, by using the full interaction between the molecules.) Thus we are not aiming at a quantitatively accurate model of the system, but this simplification enables us to compute with much better statistics. Note that for lower N_2 concentrations these permanent electrical quadrupoles do not play such an essential role, since they do not couple to the electrical neutral Ar atoms, which have no permanent electrical

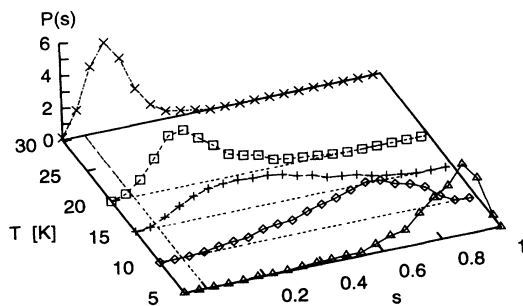


FIG. 1. Evolution of the order parameter distribution function $P_{x=0.33}(\sigma)$ with the temperature as deduced from classical MC simulation.

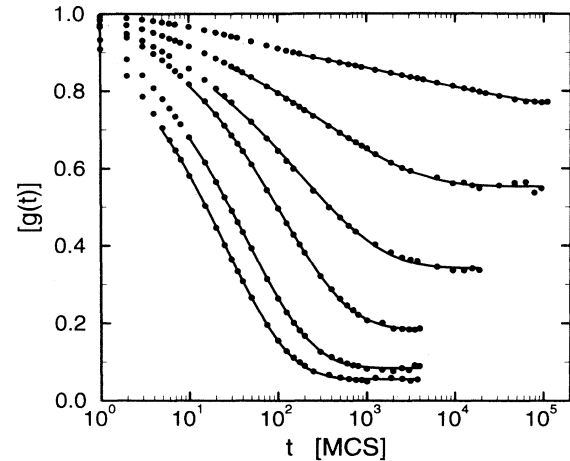


FIG. 2. Time correlation function $g_{EA}(t)$ for the temperatures $T = 5, 10, 15, 20, 30, 40$ K (from the top to the bottom). Circles refer to MC data; lines represent fits according to Eq. (2).

multipole moment. In a later study, we plan to consider this transition, focusing on the transition region. More convenient potentials will be used to do this.

We now consider the case of $x = 0.33$. The distribution of σ is peaked around zero for temperatures above $T = 30$ K. With decreasing temperature the peak of the distribution shifts gradually to larger values without any apparent discontinuity; see Fig. 1. This behavior and the fact that the specific heat has no anomaly lead to the conclusion that the system under consideration has no phase transition into a long-ranged disordered phase with local $Pa3$ -type ordering of the N_2 molecules. However, the simulated freezing of the orientational degrees of freedom is in a good qualitative agreement with the experimentally observed one for hcp lattices of the mass centers and a concentration $x = 0.66$.⁴ Clearly the real distribution is broadened by the finite observation time, so that slightly negative values of σ are detected. This, however, is only a statistical effect.

The site-averaged correlation function $g_{EA}(t) = [g_i(t)]_{av}$, whose plateau value for $\lim_{t \rightarrow \infty}$ gives σ_{EA} , contains two further important points: (i) It can be seen whether or not the samples had been equilibrated. (ii) The form of the relaxation functions gives information about the cooperativity of the reorientational motion. In Fig. 2, it can be observed that equilibration took place for

TABLE I. Relaxation time τ in MC steps and Kohlrausch exponent β for different concentrations and different temperatures; see Eq. (2).

T [K]	$\tau_{x \ll 1}$	$\beta_{x \ll 1}$	$\tau_{x=1/3}$	$\beta_{x=1/3}$	$\tau_{x=2/3}$	$\beta_{x=2/3}$
5	630	0.80	2800	0.23	$>10^4$	<0.20
10	140	0.84	340	0.40	1900	0.25
15	74	0.78	180	0.45	340	0.37
20	48	0.79	110	0.56	140	0.50
30	25	0.71	43	0.58	46	0.56
40	16	0.68	21	0.59	27	0.58

all temperatures investigated. The correlation functions, fitted by a Kohlrausch law

$$g_{EA}(t) = \sigma_{EA} + (1 - \sigma_{EA})e^{-(t/\tau)^\beta}, \quad (2)$$

become broader with decreasing temperature, indicating an increasing cooperativity. This cooperativity, expressed by a small value of the Kohlrausch exponent β , increases with increasing number of N_2 concentration; see Table I. The relatively small values of β for the dilute case $x \ll 1$ at high temperatures is not a sign of cooperativity. If the thermal energies are comparable or higher than the free energy barriers, the motion between different stable states is not activated and therefore the description of a relaxation process by an exponential is not appropriate.¹⁹ In the case of an isolated N_2 impurity in an Ar crystal the free energy barrier is of the order of $15k_B K$.²⁰ The increased collectivity of the reorientational motion presents itself in an increased relaxation time τ with decreasing temperature and increasing N_2 concentration. Even the ratios $\tau_{x_1 > x_2} / \tau_{x_2}$ grow when the temperature is lowered, indicating larger correlation lengths of systems with higher N_2 concentrations. The question arises whether or not a long-ranged disordered phase with local $Pa3$ symmetry will be the thermal state for very low temperatures.

It is very instructive to compare σ_{EA} for all systems under consideration; see Fig. 3. The pure system shows the above mentioned thermodynamic transition from disordered fcc to the ordered $Pa3$ phase. The line describing the pure system has been obtained by a fit to the computed data on the basis of a Landau-type approach. For the dilute limit, $x \rightarrow 0$, we postulate a kinetic transition for the classical system, because the energy barrier of the reorientational motion of an isolated N_2 becomes infinitely large in comparison to the thermal energy. At finite temperatures, the molecules move in between the three stable oriented states, parallel to the x , y , and z axes of the surrounding Ar crystal.^{20,21}

For the mixed systems we also postulate the value $\sigma(T = 0 \text{ K}) = 1$. All other values for σ_{EA} have been

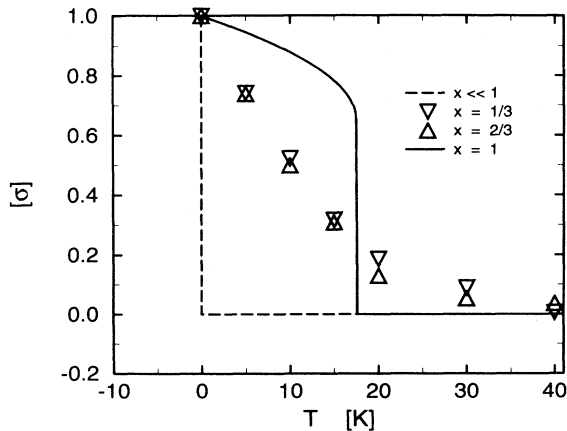


FIG. 3. Site-averaged order parameter for various N_2 concentrations. Error bars are smaller than the symbol size.

obtained numerically and only in the case of $x = 2/3$ and $T = 5 \text{ K}$ did the plateau value have to be obtained by extrapolating the measured correlation function. The manner in which σ_{EA} tends to 1 with decreasing temperature for the mixed systems differs clearly from the case where a kinetic or a thermodynamic transition is found. Also the specific heat show three types of different behaviors. The thermodynamic transition is accompanied by a singularity in the specific heat at the transition temperature. In the classical case of the dilute system there is no maximum observable and in the case of the mixed systems we observed a small relative maximum at $T \approx 15 \text{ K}$. This coincides with the temperature region where the order parameter begins to grow considerably and it coincides with the free energy barrier (over k_B) separating the three stable orientational states in the dilute case.

The orientation correlation function $P_{NN}(\vec{n}_i \cdot \vec{n}_j)$, which gives the probability of the scalar product of the directors of two neighbored N_2 molecules, can indicate whether the freezing in process of fcc $Ar_{1-x}(N_2)_x$ with $x < x_c$ is related to the fcc to $Pa3$ transition. In Fig. 4 we plot the site-averaged $P_{NN}(\vec{n}_i \cdot \vec{n}_j)$. It turns out that the short-range order in the mixed crystal prefers parallel directors of the molecules, while for the pure system $\cos(\gamma) = 1/3$ is preferred for $T < T_1$, according to the $Pa3$ symmetry and for $T > T_1$ a nearly constant distribution is found for $\cos(\gamma)$ in the pure case.

We conclude that even in cubic $Ar_{1-x}(N_2)_x$ an orientational glass state can be found that is not related to the $Pa3$ reference phase. The preferred parallel alignment of N_2 molecules in mixed $Ar_{1-x}(N_2)_x$ crystals may explain the orthorhombic distortion of hcp $Ar_{1-x}(N_2)_x$ found by Klee and Knorr¹³ as well as an anomaly in the mechanical modulus C_{11} in mixed $Ar_{1-x}(N_2)_x$ found by Westerhoff *et al.*,²³ while usually a perpendicular alignment of neighbored rotators leads to anomalies in C_{44} .²⁶

In order to quantify quantum effects, path integral Monte Carlo simulations²⁵ have been carried out for $x = 0.33$ and $T = 20 \text{ K}$. On the one hand T is already well

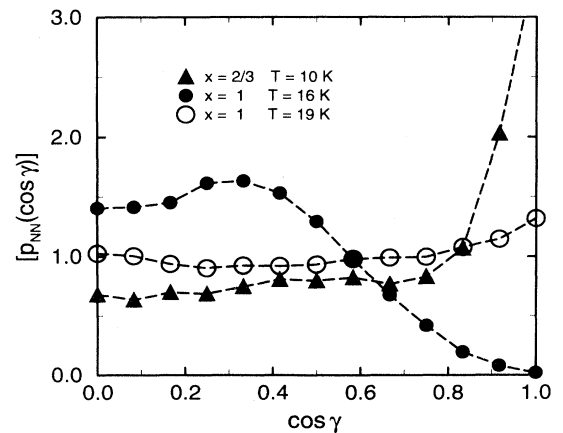


FIG. 4. Site-averaged orientation correlation function $P_{NN}(\vec{n}_i \cdot \vec{n}_j)$ for the pure system 10% above and 10% below the transition temperature and for the mixed system $x = 2/3$ at $T = 10 \text{ K}$.

below the Debye temperature T_D of both pure systems; on the other hand it is still easy to reach the quantum limit by a suitable simulation method. The translational degrees of freedom were treated quantum mechanically with a Trotter number $P = 10$. With this choice of P and T , the quantum limit is nearly reached, because $PT \approx 2T_D$. The orientational degrees of freedom have been treated classically. The influence of quantizing the orientational degrees of freedom on real space correlation functions and the influence of lattice distortions on internal rotational quantum states have been discussed elsewhere.^{24,21} The peaks in the Ar-Ar spatial correlation functions are broadened by quantum effects and by disorder effects. At a temperature $T = 20$ K the nearest neighbor peaks are broadened mainly due to the quantum nature of the particles. For next nearest neighbors the amount of the broadening due to quantum and disorder effects is nearly identical and for the fourth nearest neighbors quantum and classical distributions coincide. The effect of decreasing the quantum influence with increasing distance may be explained by the fact that low wave number Fourier components corresponding to (more classically) low-energy excitations are responsible for the long-distance effects. Due to the center of mass quantum delocalization the N_2 orientational degrees of freedom are more strongly localized, resulting in a 9% increase of $\sigma_{EA} = 0.214$ compared to a classical treatment, where $\sigma_{EA} = 0.197$.

In order to quantify the effects of the translational rotational coupling, we performed a comparative study of the system with the same parameters as in the last paragraph, but fixing all translational degrees of freedom to their fcc lattice points. This results in a stronger reduction of the order parameter to $\sigma_{EA} = 0.104$ and a reduction of the correlation time of about 50%. These effects can presumably be attributed to the two points: (i) Some of the N_2 molecules have only Ar atoms as nearest neighbors and therefore the rotational potential has nearly cubic symmetry, resulting in the local order parameter being zero. (ii) Translational rotational coupling leads to an effective longer-ranged interaction of two N_2 molecules, compared to the case with fixed translational degrees of freedom. Therefore the number of interacting molecules is reduced in the latter case, resulting in a smaller collectivity and thus in a reduced correlation time and order parameter.

We thank K. Binder and K. Knorr for useful discussions. This research was carried out in the framework of the Sonderforschungsbereich 262 der Deutschen Forschungsgemeinschaft. P.N. thanks the DFG for financial support (Heisenberg foundation). The computations were carried out on the CRAY YMP of the HLRZ at Jülich.

-
- ¹ U.T. Höchli, K. Knorr, and A. Loidl, *Adv. Phys.* **39**, 409 (1990).
² K. Binder and J.D. Reger, *Adv. Phys.* **41**, 547 (1992).
³ D. Hammes, H.-O. Carmesin, and K. Binder, *Z. Phys. B* **76**, 115 (1989).
⁴ D. Esteve, N.S. Sullivan, and M. Devoret, *J. Phys. Lett.* **43**, 793 (1982).
⁵ A.B. Harris and H. Meyer, *Can. J. Phys.* **63**, 3 (1985).
⁶ X. Li, H. Meyer, and A.J. Berlinski, *Phys. Rev. B* **37**, 3216 (1988).
⁷ M. Devoret and D. Esteve, *J. Phys. C* **16**, 1827 (1983).
⁸ M. Scheucher, J.D. Reger, K. Binder, and A.P. Young, *Phys. Rev. B* **42**, 6881 (1990).
⁹ P.C.W. Holdsworth, M.J.P. Gingras, B. Bergersen, and E.P. Chan, *J. Phys. Condens. Matter* **3**, 6679 (1991).
¹⁰ $\epsilon_{Ar-Ar} = 121k_B K$, $\sigma_{Ar-Ar} = 3.40 \text{ \AA}$, $\epsilon_{N-N} = 37.3k_B K$, $\sigma_{N-N} = 3.31 \text{ \AA}$, $\epsilon_{Ar-N} = (\epsilon_{Ar-Ar}\epsilon_{N-N})^{1/2}$, $\sigma_{Ar-N} = (\sigma_{Ar-Ar}\sigma_{N-N})^{1/2}$; diameter of the N_2 molecule: 0.545 \AA .
¹¹ D.H. Klee, H.O. Carmesin, and K. Knorr, *Phys. Rev. Lett.* **61**, 1855 (1988).
¹² C.S. Barrett and L. Meyer, *J. Chem. Phys.* **42**, 107 (1965).
¹³ H. Klee and K. Knorr, *Phys. Rev. B* **42**, 3152 (1990).
¹⁴ F. Silvera, *Rev. Mod. Phys.* **52**, 393 (1980).
¹⁵ H. Klee and K. Knorr, *Phys. Rev. B* **43**, 8658 (1991).
¹⁶ J. De Kinder, E. Goovaerts, A. Bouwen, and D. Schoemaker, *Phys. Rev. B* **44**, 10369 (1991).
¹⁷ R.S. Pfeiffer and G.D. Mahan, *Phys. Rev. B* **48**, 669 (1993).
¹⁸ J. Belak, R. Le Sar, and R.D. Eppers, *J. Chem. Phys.* **92**, 5430 (1990).
¹⁹ D. Chandler, *J. Chem. Phys.* **68**, 2959 (1978).
²⁰ M.H. Müser and G. Ciccotti, *J. Chem. Phys.* (to be published).
²¹ M.H. Müser, W. Helbing, P. Nielaba, and K. Binder, *Phys. Rev. E* **49**, 3956 (1994).
²² J.R. Cullen, D. Mukamel, S. Shtrikman, L.C. Levitt, and E. Callen, *Solid State Commun.* **10**, 195 (1972).
²³ T. Westerhoff, F. Bruchhäuser, R. Feile, and R. Boehler, *J. Non-Cryst. Solids* **172-174**, 481 (1994).
²⁴ W. Helbing, P. Nielaba, and K. Binder, *Phys. Rev. B* **44**, 4200 (1991).
²⁵ M.H. Müser, P. Nielaba, and K. Binder, *Phys. Rev. B* **51**, 2723 (1995).
²⁶ R.M. Lynden-Bell and K.H. Michel, *Rev. Mod. Phys.* **66**, 721 (1994).